Energy Conversion and Management 60 (2012) 125–133

Contents lists available at SciVerse ScienceDirect

Energy Conversion and Management

journal homepage: www.elsevier.com/locate/enconman

Optimization of thermoelectric heat pumps by operating condition management and heat exchanger design

Benjamin David, Julien Ramousse, Lingai Luo *

LOCIE, CNRS UMR 5271, Université de Savoie, Campus Scientifique, Savoie Technolac, 73376 Le Bourget du Lac, France

ARTICLE INFO

Article history:
Available online 27 March 2012

Keywords:
Thermoelectric heat pump
Heat exchangers
Optimization
Analytical model
COP maximization
Entropy generation minimization

ABSTRACT

This paper introduces an optimization method for improving thermoelectric heat pump performance by operating condition management of the thermoelectric modules (TEMs) and design optimization of the heat exchangers linked to the TEMs. The device studied, corresponding to an original configuration of the thermoelectric heat pump, comprises two commercial thermoelectric modules and two mini-channel heat sinks through which water flows, in contact with both sides of the TEMs. The objective function is the maximization of the device's coefficient of performance (COP), including the electrical and mechanical consumption of the thermoelectric modules and the circulating auxiliaries. First, the optimization variables are the number and the diameter of mini-channels, and the mass flows for both heat sinks (hot and cold sides). The results show that similar results are obtained by minimization of the entropy generation in the device. Finally, the hot thermal power demand is included in the optimization variables for complete optimization of the device. The results of full optimization converge with those obtained with the previous partial optimization.

1. Introduction

Thermoelectric heat pumps are devices that exploit the temperature difference created by the Peltier effect between the junctions of semi-conductors. Thermoelectric phenomena [1–3] were observed and described during the first half of the 19th century. However, because of the low figure of merit characterizing the quality of the thermoelectric material used at this time, the thermoelectric effect was mainly exploited for measuring high temperatures. In 1885, Rayleigh proposed creating a thermoelectric generator [4], but the first real application only appeared in 1947 with the Telkes thermoelectric generator [5]. During the period from 1957 to 1965, many thermoelectric materials were discovered, notably bismuth telluride, which shows the highest figure of merit at ambient temperature [6]. Today, this material is still the most widely used for applications at ambient temperature. In a thermoelectric heat pump, the two important characteristics are the quality of the material used and the thermal resistances of the device. Many studies have been conducted on the optimization of the thermoelectric device; however, most of them deal with only one part of the device, such as the thermoelectric elements [7–9], the contact thermal resistance [7], or the influence of the heat exchangers [10,11]. Crane and Jackson [12] also worked on the optimization of cross-flow heat exchangers coupled to a thermoelectric module with the ratio between the useful thermal power and the cost of the device as the objective function. Khire et al. [13] worked on the optimization of a thermoelectric heat pump coupled to a building. The optimization simultaneously minimizes two design objectives, the input power and the number of thermoelectric modules. In this study, a method based on coupling the thermoelectric phenomena to heat transfer and pressure drop phenomena in the heat exchangers is proposed to optimize a thermoelectric heat pump operating with water. This method allows precise determination of the optimal geometrical dimensions of the heat exchangers and the optimal operating conditions for given fluid temperatures. The objective function considered is the device's coefficient of performance (COP) including the mechanical consumption of the circulating auxiliaries. Design, mass flows and electrical power are considered as optimization variables. Finally, the results obtained are compared with a second objective function: the minimization of entropy generation. The potential application concerns heating and cooling in low-consumption buildings.

2. Configuration of the device

The thermoelectric heat pump unit considered in this study comprises three heat exchangers and two thermoelectric modules. This thermoelectric heat pump configuration results from a previous study on an optimized method of thermoelectric heat pump management designed to increase the global performance of the device [14]. This study showed that it is possible to maintain an

* Corresponding author. Tel.: +33 479758193; fax: +33 479758144.
E-mail address: lingai.luo@univ-savoie.fr (L. Luo).

0196-8904/$ - see front matter © 2012 Elsevier Ltd. All rights reserved.
doi:10.1016/j.enconman.2012.02.007

Nomenclature

A	surface area, m^2
Cp	specific heat, J Kg^{-1} K^{-1}
D	diameter, m
E	space between two channels, m
f	friction factor
h	heat transfer coefficient, W m^{-2} K^{-1}
H	height, m
I	electrical intensity, A
K	thermal conductance, W K^{-1}
L	length, m
$\dot{m}$	mass flow, Kg s^{-1}
N	number of channels
Nu	Nusselt number
P	pressure
Pr	Prandtl number
R	resistance, K W^{-1}
Re	Reynolds number
S	entropy, W K^{-1}
T	temperature, K
v	velocity, m s^{-1}

Greek symbols

α	Seebeck coefficient, V K^{-1}
λ	thermal conductivity, W m^{-1} K^{-1}
ϕ	power, W
ρ	density, Kg m^{-3}

Subscripts

c	cold
elec	electrical
gen	generate
h	hot
opt	optimal
m	mechanical
device	relative to the complete device

Superscripts

b	bulk
cer	ceramic
ctc	contact
ch	channel
cond	conductivity
conv	convection
f	fluid
in	inlet
int	interface
j	junction
out	outlet
tot	total
opt	optimal
TEM	thermoelectric module

optimal COP of the device for given temperature conditions using parallel and cascade associations for any thermal power needed. The configuration presented in Fig. 1 illustrates a parallel operating mode. Heat transfer is mainly ensured by convection in the working fluid. In this configuration, the same mass flow for the two cold heat exchangers and the same electrical intensity supplied for both TEMs are assumed. Finally, the hot heat exchanger dissipates the same thermal power on its two sides.

Fig. 2 illustrates the same device presented in Fig. 1 in cascade operating mode. In this configuration, the two TEMs are associated in cascade and the thermal flux is transferred from the cold heat exchanger to the hot heat exchanger via thermal conduction through the central heat exchanger. The working fluid does not flow through the hot heat exchanger. This configuration allows increasing the maximal COP with a reduction of the corresponding thermal power. Consequently, the heat exchanger studied here is original because two operating modes are considered: conduction through the bulk when the thermoelectric modules are associated in cascade and convection when the thermoelectric modules are associated in parallel. This original heat exchanger is covered by patent FR 11 53394.

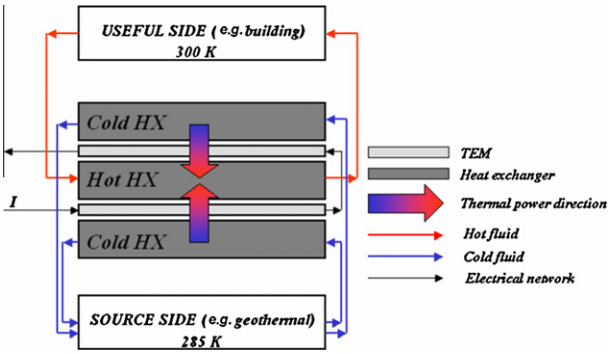

Fig. 1. Scheme of the device for a parallel mode.

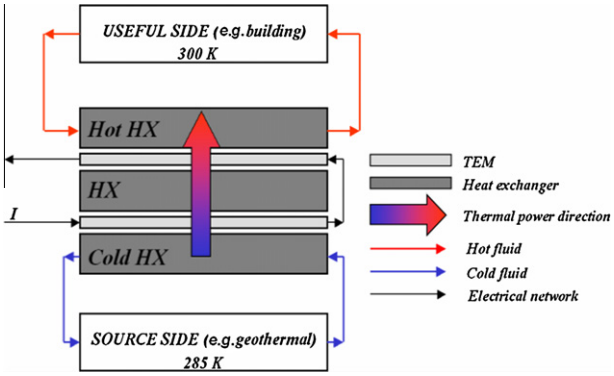

Fig. 2. Scheme of the device for a cascade mode.

Heat transfer by conduction in heat exchangers (cascade) is less restrictive than by convection (parallel); consequently, this study focuses on the parallel mode. Therefore the method introduced here aims to optimize the design of the heat exchangers and the operating conditions for the parallel operating mode.

Only the heating mode is considered here. The hot and cold fluid temperatures are respectively set to 300 K and 285 K (Fig. 1), corresponding to floor heating temperature in the building and to a constant geothermal source, respectively. These operating temperatures are kept constant in the following in order to validate the optimization approach.

3. Analytical model

The goal of this study is to optimize the performance of a thermoelectric heat pump device. The optimization method must

integrate thermoelectric phenomena into the thermoelectric module as well as heat transfers and pressure drops in the heat exchangers. First, a description of the analytical model used in this paper is presented. Based on this model, the optimization of the heat sink design (D^{ch},N^{ch}) and the operating conditions ($\dot{m}_c^{tot}$, $\dot{m}_h^{tot}$, ϕ_h) is discussed in the next section.

3.1. Thermoelectric phenomena

In 1834, Jean Peltier, a French physicist, discovered that an electrical current flowing through the junctions between dissimilar materials causes a temperature difference. Finally, absorption of thermal power ϕ_c at the cold junction and generation of thermal power ϕ_h at the hot junction are observed. These two thermal powers are defined as [15]:

$$\phi_h = \alpha I T_h^j + \frac{1}{2} R_{elec} I^2 - K(T_h^j - T_c^j) \quad (1)$$

$$\phi_c = \alpha I T_c^j - \frac{1}{2} R_{elec} I^2 - K(T_h^j - T_c^j) \quad (2)$$

The electrical power to supply at the thermoelectric module is the difference between the hot and cold thermal powers.

$$\phi_{elec} = \phi_h - \phi_c = \alpha I(T_h^j - T_c^j) + R_{elec} I^2 \quad (3)$$

The performance of thermoelectric modules is characterized by the COP, which is defined as the ratio between the useful thermal power released and the electrical power supplied. In heating mode, the useful thermal power is the hot thermal power and the source thermal power is the cold thermal power. It is the opposite in cooling mode. Finally, depending on the mode considered two COPs can be written:

$$COP_h^{TEM} = \frac{\phi_h}{\phi_{elec}} = \frac{\phi_c}{\phi_{elec}} + 1 = COP_c^{TEM} + 1 \quad (4)$$

As shown by Eqs. (1)–(4), the performance of a thermoelectric device is a direct function of the material's properties (α, R_{elec} and K), the electrical intensity supplied I and the junction temperatures T_h^j and T_c^j. The material's properties used in this study are provided by Ferrotec [16] and correspond to bismuth telluride:

$$\alpha = 0.101 \text{ V K}^{-1} \quad (5)$$

$$R_{elec} = 1.7352\ \Omega \quad (6)$$

$$K = 2.6637 \text{ W K}^{-1} \quad (7)$$

Fig. 3 plots the variation of COP versus the hot thermal power demand, for different temperature differences (with $T_c^j = 285$ K). It clearly shows that for a given temperature difference, an optimal hot thermal power ϕ_h^{opt} exists, leading to the maximal COP. As a consequence, an optimal electrical intensity I^{opt} exists, leading to the maximal COP. The greater the difference in junction temperature is, the lower the maximal COP and the higher the corresponding optimal hot thermal power.

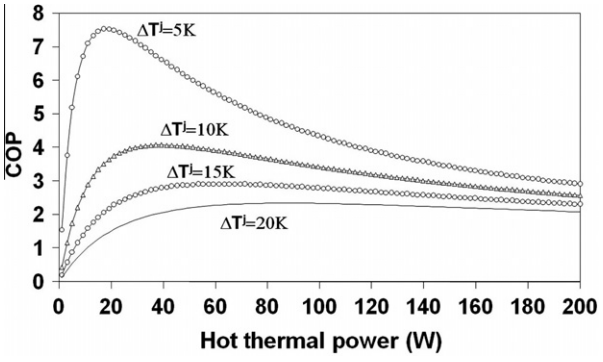

Fig. 3. COP as a function of the hot thermal power for different junction temperature differences.

3.2. Heat transfer in the heat exchangers

3.2.1. Heat exchanger design

The heat exchangers linked to the hot and cold junctions are identical to ensure the reversibility of the device (heating or cooling mode). They are made up of parallel circular mini-channels with a global "Z" configuration. In 1996, Kikas [17] demonstrated that this configuration provides a good distribution of the thermal fluxes on the entire heat exchanger area. In fact, a good distribution of the thermal fluxes provides the same temperature conditions for all the semi-conductor junctions. Finally, the optimal intensity supplied to the TEM is optimal for all the semi-conductor junctions.

The calorific fluid used is water and the thermal conductivity of the heat exchangers' material is $\lambda = 237 \text{ W m}^{-1} \text{ K}^{-1}$ (aluminum). The surface area (LL) occupied by the mini-channels corresponds to the thermoelectric module area considered (Fig. 4).

Thus, the geometrical constraints enforce:

$$D^{ch} = \frac{L - (N^{ch} E)}{N^{ch}} \quad (8)$$

The height H corresponding to the thickness of the heat exchanger bulk is set to 3 mm for this study.

One of the weaknesses of this kind of design stems from the flow distribution. In fact, many studies have shown that in this configuration, a nonuniform distribution of the different mass flow in the mini-channel is observed [18–21]. These studies illustrate that the greater the diameter of the distributor and the collector, the better the flow distribution is. We can also note that the distribution depends to a large extent on the number of mini-channels and the Reynolds number.

A fluidic model was built and integrated into the global model introduced in this study in order to integrate and analyze the effects of maldistribution in the mini-channels on the device's global COP. Due to the complexity of the problem, this aspect will not be presented in detail in this paper. However, a complementary study has shown that the collector and distributor diameters must be set at 15 mm to obtain uniform distribution of the fluid in all the mini-channels. Consequently, it can be written:

$$\dot{m}_{h/c}^{ch} = \frac{m_{h/c}^{tot}}{N^{ch}} \quad (9)$$

To keep the same temperature difference from the inlet to the outlet of both heat exchangers, the mass flows for each side differ due to the thermal power difference between the hot and cold sides (Eqs. (1) and (2)).

The boundary conditions of the problem are presented in Fig. 5. The thermal fluxes are transferred on both sides of the central heat exchanger. Finally, for symmetry reasons the study domain is reduced to one mini-channel on its half height for the hot side.

3.2.2. Thermal resistances

The total thermal resistances $R_{h/c}^{tot}$ from the junction to the fluid can be divided into three distinct thermal resistances related to the thermal conduction through the bulk of the heat exchanger, the convective heat transfer in the mini-channels and the heating of the fluid. Finally, the total thermal resistances for the hot and cold sides are:

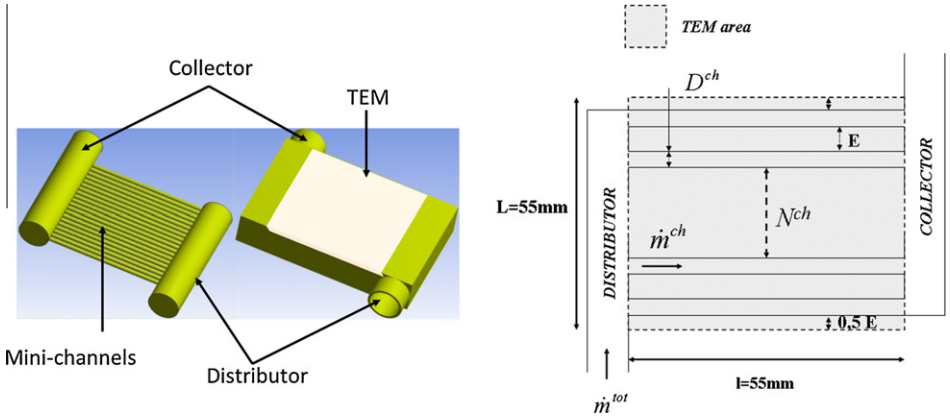

Fig. 4. Heat exchanger design.

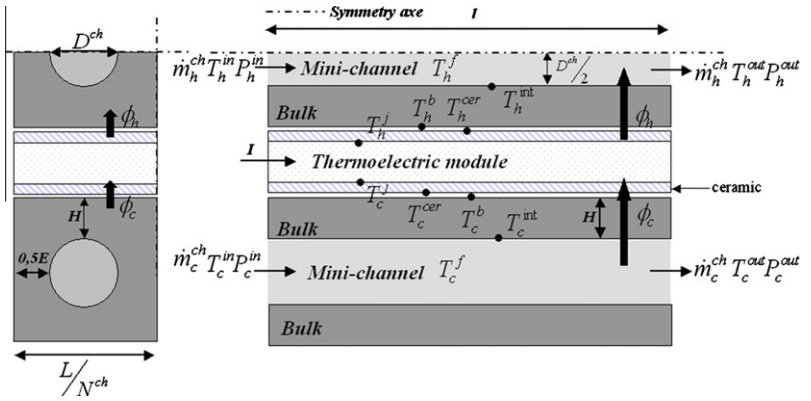

Fig. 5. Boundary conditions of the problem.

$$R_h^{tot} = \frac{T_h^j - T_h^{in}}{\phi_h} = \frac{T_h^j - T_h^{cer}}{\phi_h} + \frac{T_h^{cer} - T_h^b}{\phi_h} + \frac{T_h^b - T_h^{int}}{\phi_h} + \frac{T_h^{int} - T_h^f}{\phi_h} + \frac{T_h^f - T_h^{in}}{\phi_h} \quad (10)$$

$$R_h^{tot} = R^{cer} + R^{ctc} + R^{cond} + R_h^{conv} + R_h^f \quad (11)$$

$$R_c^{tot} = \frac{T_c^{out} - T_c^j}{\phi_c} = \frac{T_c^{cer} - T_c^j}{\phi_c} + \frac{T_c^b - T_c^{cer}}{\phi_c} + \frac{T_c^{int} - T_c^b}{\phi_c} + \frac{T_c^f - T_c^{int}}{\phi_c} + \frac{T_c^{out} - T_c^f}{\phi_c} \quad (12)$$

$$R_h^{tot} = R^{cer} + R^{ctc} + R^{cond} + R_h^{conv} + R_h^f \quad (13)$$

The thermal resistance due to the conduction through the bulk of the heat exchanger is estimated as follows:

$$R^{cond} = \frac{H}{\lambda A} \quad (14)$$

The thermal constriction resistances due to the circular geometry of the channel are not considered in this study. Consequently, thermal transfer through the bulk of the heat sink is assumed to be one-dimensional. This assumption is acceptable because the constriction resistance must be negligible in the conduction resistance with regard to heat exchanger dimensions (H = 6 mm and D^{ch} = 0.6 mm). Moreover, we show that the convective resistance is the main part of the total thermal resistance (see Fig. 10). The convective thermal resistance between the wall of the mini-channel and the fluid flow is different for the heat exchanger through which the cold fluid flows and the heat exchanger through which the hot fluid flows. In fact, the hot heat exchanger at the center of the device has to dissipate two thermal fluxes coming from its two opposite sides. Finally, we can consider that the exchange area between the solid and the fluid for the central heat exchanger is half of the exchange area of the two heat exchangers at the extremity of the device:

$$R_h^{conv} = \frac{2}{h_h A^{int}} \quad (15)$$

$$R_c^{conv} = \frac{1}{h_c A^{int}} \quad (16)$$

with $h_{h/c}$, the convection coefficient equals:

$$h_{h/c} = \frac{Nu_{h/c}\lambda}{D^{ch}} \quad (17)$$

and the Nusselt number (for 0.7 < Pr < 7 and Re < 2300) equals [22]:

$$Nu_{h/c} = 4.364 + \frac{0.086\left(Re_{h/c} Pr \frac{D^{ch}}{L}\right)^{1/3}}{1 + 0.1Pr\left(Re_{h/c}\frac{D^{ch}}{L}\right)^{0.83}} \quad (18)$$

This correlation assumes that the thermal flux is circumferentially uniform around the mini-channel. This assumption is not fully verified, even for the central heat sink. A complementary study has to be carried out to evaluate the heat transfer coefficient precisely.

However, this correlation is used to estimate an effective average Nusselt in the channel in this paper. The optimal results may

be slightly different estimating the convective heat transfer coefficient differently, but the approach proposed in this paper remains valid.

The thermal resistance linked to the heating of the fluid from the inlet $T^{in}_{h/c}$ to the mean fluid temperature in the channel $T^{f}_{h/c}$ is:

$$R^{f}_{h/c} = \frac{2}{\dot{m}^{tot}_{h/c} Cp} \tag{19}$$

As $T^{f}_{h/c}$ is the mean temperature of the fluid between the inlet and the outlet of the mini-channel, a factor of 2 appears.

The analytical model also includes the thermal resistances coming from the ceramics of the TEM and the contact between the TEM and the bulk of the heat exchangers from [16,23].

$$R^{cer} = 0.014 \text{ K W}^{-1}$$

$$R^{ctc} = 0.003 \text{ K W}^{-1}$$

3.2.3. Pressure drop

Correlations used for the calculation of the pressure drops are a function of the development length, defined as [24]:

$$L^{in}_{h/c} = 0.05 \mathrm{Re}_{h/c} D^{ch} \tag{20}$$

For the inlet region, we have (for Re < 2300) [25]:

$$\frac{\Delta P_{h/c}}{0.5 \rho v^2_{h/c}} = 13.74 (x^{+}_{h/c})^{1/2} + \frac{1.25 + 64 x^{+}_{h/c} - 13.74 (x^{+}_{h/c})^{1/2}}{1 + 0.00021 (x^{+}_{h/c})^{-2}} \tag{21}$$

with

$$x^{+}_{h/c} = \frac{l/D^{ch}}{\mathrm{Re}_{h/c}} \quad \text{if } L^{in}_{h/c} > l \quad \text{and} \quad x^{+}_{h/c} = \frac{L^{in}_{h/c}/D^{ch}}{\mathrm{Re}_{h/c}} \quad \text{if } L^{in}_{h/c} < l \tag{22}$$

For the fully developed region, we have [26,27]:

$$\Delta P_{h/c} = f_{h/c} \left(\frac{(l - L^{in}_{h/c}) v^2_{h/c} \rho_f}{2 D^{ch}} \right) \tag{23}$$

with

$$f_{h/c} = \frac{64}{\mathrm{Re}_{h/c}} \tag{24}$$

The singular pressure drops due to the bifurcation of the fluid from the distributor to the channels as well as the confluence of the fluid from the channels to the collector are not treated in this study. A complementary fluidic model including all the flow distribution phenomena helps estimate the error caused by this assumption. The error reported is about 20%, so that singular pressure drops are ignored to reduce the complexity of the model. The authors are aware that the error induced by this assumption may modify the optimal design. However, the increase in total pressure drop influences the optimal geometry of the heat exchanger very slightly, as reported in [28].

Finally, the total mechanical consumption of the two fluid circulating auxiliaries (assuming a pump efficiency of 1) corresponds to:

$$\phi_m = \frac{\dot{m}^{tot}_h \Delta P_h + 2 \dot{m}^{tot}_c \Delta P_c}{\rho} \tag{25}$$

As described in Fig. 1, there is one heat exchanger at the center of the device through which the hot fluid flows and the two heat exchangers at the extremity through which the cold fluid flows.

4. Thermoelectric heat pump optimization

The two junction temperatures calculated with the thermoelectric model are linked to the useful and source fluid temperatures (T^{f}_{h} and T^{f}_{c}) via the thermal resistances of the heat exchangers.

$$\phi_h = \frac{T^{j}_{h} - T^{f}_{h}}{R^{tot}_{h}} \tag{26}$$

$$\phi_c = \frac{T^{f}_{c} - T^{j}_{c}}{R^{tot}_{c}} \tag{27}$$

Fluid temperatures are the known inputs in a thermoelectric heat pump (rather than the junction temperatures, which are most often used in the literature). Eqs. (26) and (27) explicitly show that the thermal resistances of the heat exchangers highly influence the junction temperatures and therefore the device performance. Indeed, Fig. 6 introduces the temperature profiles along the thermoelectric heat pump. It is shown that the lower the thermal resistance, the lower the temperature difference between the junctions is, resulting in increasing the COP (see Fig. 3).

To sum up, the COP of a TEM integrated into a thermoelectric heat pump is a direct function of the electrical intensity (see Fig. 1) supplied and of the heat exchanger thermal resistances linking the junction temperature to the fluid temperature. The goal of this study is to optimize the device's global COP, including the pressure drop in the heat exchangers. The device's COP is defined as:

$$\mathrm{COP}_{device} = \frac{\phi_h}{\phi_{elec} + \phi_m} \tag{28}$$

Finally, to optimize the device we need to optimize both the heat exchanger design (N^{ch}, D^{ch}) and the operating conditions (I^{opt}, $\dot{m}^{tot}_{h/c}$).

First, optimization for a given thermal power demand is handled with two different objective functions and then complete optimization including the hot thermal power as a complementary optimization variable of the device is presented. The direct search method [29] is used with the Engineering Equation Solver (EES) software.

4.1. Optimization for a fixed thermal power demand

First let us consider a case with a fixed thermal power demand. The optimization problem can be handled by maximizing the device's COP. The optimization variables are the mass flows for the cold and hot sides, the channel diameter and the number of channels.

$$\max_{X \in \mathbb{R}^4} \mathrm{COP}_{device}(X) \in \mathbb{R} \tag{29}$$

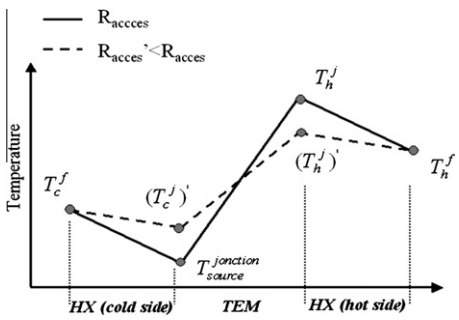

Fig. 6. Influence of the thermal resistances on the junction temperatures.

$$X = (D^{ch},\ N^{ch},\ \dot{m}_c^{tot},\ \dot{m}_h^{tot}) \tag{30}$$

Subjected to:

$$E > 0.0002\ \text{m} \tag{31}$$

$$D^{ch} > 0.0002\ \text{m} \tag{32}$$

$$\Delta T_h^f = \Delta T_c^f \tag{33}$$

Parameters E and D^{ch} are constraints due to the limit of the manufacturing process. The optimization results show that whatever the useful thermal power, the optimal value of E corresponds to the lower bound. A constant temperature difference between the hot and cold sides is assumed, as has been explained in Section 3.2.1. Fig. 7 shows that the optimal number of channels decreases with the increase of the hot thermal power demand. As a consequence, and due to the fact that E is constant and equal to the lower bound value, the mini-channel diameter and finally the total exchange area between solid and fluid increase with the hot thermal power demand (see Eq. (8)). The optimal mass flow in each heat exchanger increases with the increase of the hot thermal power demand in order to keep the heat transfer coefficient high (Fig. 8). Finally, an increase of the optimal Reynolds number (Fig. 8) and thus the pressure drop and the heat transfer coefficient is observed when the hot thermal power increases (Fig. 9).

Fig. 10 shows the relative proportion of the convection resistance to the conduction resistance as a function of the thermal power demand. The higher the thermal power demand, the lower this ratio is. Indeed, the thermal resistance due to conduction is constant but the higher the thermal power, the higher the convective heat transfer coefficient is. The ratio is within the range of 5–8. For this reason, the controlling thermal resistance is the convection, as stated in Section 3.2.2, and the constriction resistance in the bulk can be ignored.

Fig. 11 clearly illustrates the weak influence of the mechanical consumption of the fluid-circulating auxiliaries compared to the electrical consumption of the thermoelectric modules. It helps to validate the assumption related to ignoring the singular pressure drops, stated in Section 3.2.3.

Fig. 12 illustrates the optimized COP versus hot thermal power demand. The optimal COP shows a maximum corresponding to an optimal hot thermal power demand of about 55 W (for the case considered). The changes in COP versus hot thermal power demand corresponds to the classical behavior of a thermoelectric element versus hot thermal power, as shown in Fig. 3.

One of the most widely used criteria for the optimization of the heat exchanger [30,31] and for the thermoelectric devices [32,33]

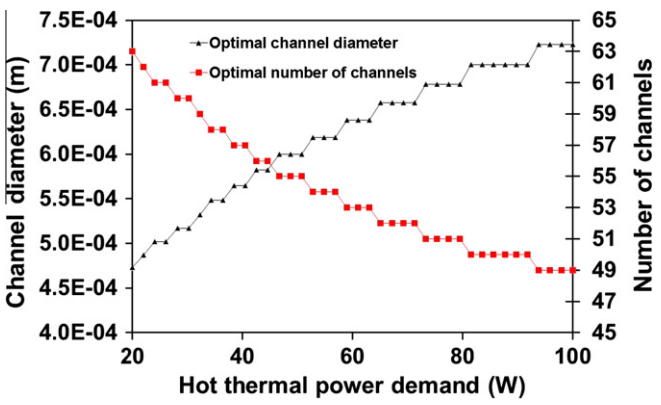

Fig. 7. Optimal number of channels and optimal channel diameter as a function of the hot thermal power demand.

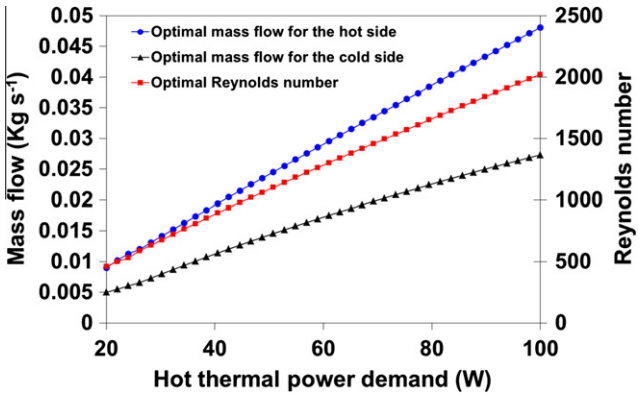

Fig. 8. Optimal mass flow for the cold and hot sides as a function of the hot thermal power demand.

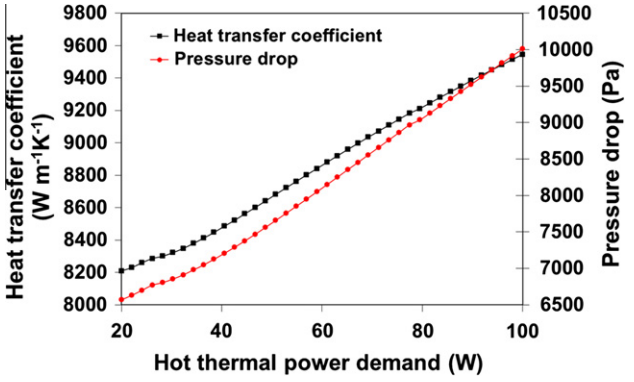

Fig. 9. Heat transfer coefficient and Reynolds number as a function of hot thermal power demand.

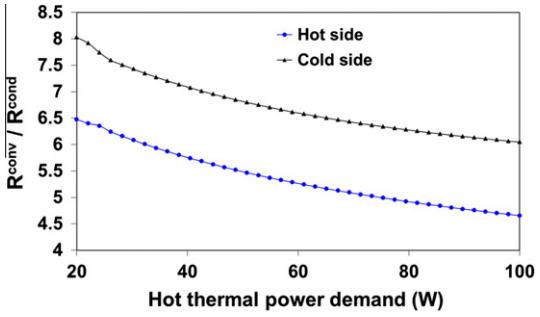

Fig. 10. Ratio between the thermal resistance due to convection and conduction as a function of hot thermal power demand.

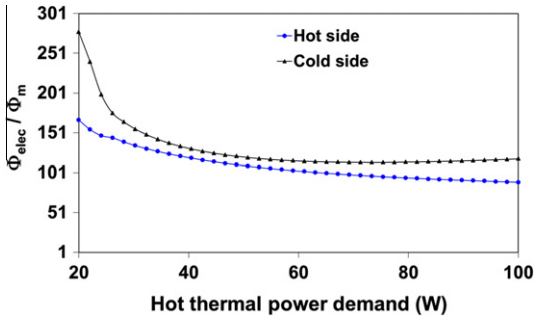

Fig. 11. Ratio between electrical consumption and mechanical consumption as a function of hot thermal power demand.

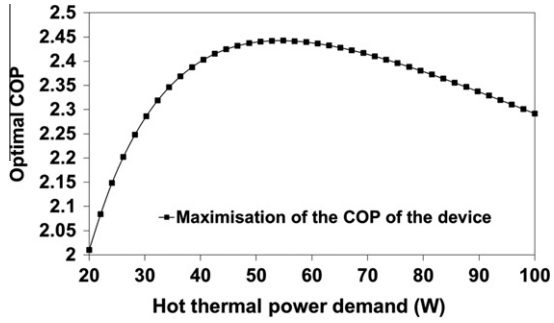

Fig. 12. Optimal COP of the device as a function of the hot thermal power demand.

has long been entropy generation minimization (EGM). For this study, an adiabatic device is considered, so the two principal entropy generation sources result from the pressure drop in the heat exchangers and the thermal transfer. The three subsystems generating entropy are described in Fig. 13.

In the thermoelectric element, the entropy generation due to thermal transfer is:

$$S_{gen}^{\mathrm{TEM}} = -\frac{\phi_c}{T_c^j} + \frac{\phi_h}{T_h^j} \tag{34}$$

For the cold and hot sides of the heat exchangers, the entropy generation is, respectively [34]:

$$S_{gen}^{c} = \frac{\phi_c}{T_c^j} + \dot{m}_c^{tot} CpLn \frac{T_c^{out}}{T_c^{in}} + \frac{\dot{m}_c^{tot} \Delta P_c}{\rho T_c} \tag{35}$$

$$S_{gen}^{h} = -\frac{\phi_h}{T_h^j} + \dot{m}_h^{tot} CpLn \frac{T_h^{out}}{T_h^{in}} + \frac{\dot{m}_h^{tot} \Delta P_h}{\rho T_h} \tag{36}$$

Finally the total entropy generation of the device is the sum of the entropy generation of each subsystem, which reduces to:

$$S_{gen}^{tot} = \dot{m}_h^{tot} CpLn \frac{T_h^{out}}{T_h^{in}} + \frac{\dot{m}_h^{tot} \Delta P_h}{\rho T_h} + \dot{m}_c^{tot} CpLn \frac{T_c^{out}}{T_c^{in}} + \frac{\dot{m}_c^{tot} \Delta P_c}{\rho T_c} \tag{37}$$

The optimization problem can thus be written:

$$\min_{X \in \mathbb{R}^4} S_{gen}^{tot}(X) \in \mathbb{R} \tag{38}$$

$$X = (D^{ch},\ N^{ch},\ \dot{m}_c^{tot},\ \dot{m}_h^{tot}) \tag{39}$$

The constraints are the same as for the maximization of the device's COP (Eqs. (31)–(33)).

Fig. 14 compares the device's COP obtained by maximizing the device's COP and by using the EGM criterion. The similarity

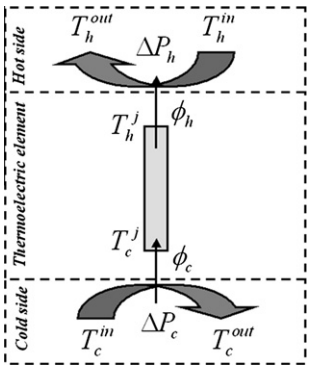

Fig. 13. Decomposition of entropy generation sources.

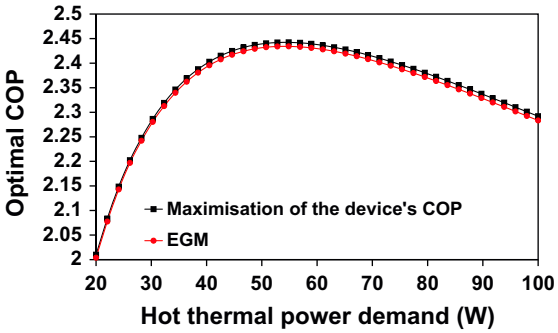

Fig. 14. Optimal COP of the device as a function of the hot thermal power demand and for two optimization criteria.

of the results between these two optimization criteria leads to concluding that:

$$\max_{X \in \mathbb{R}^4} \mathrm{COP}_{device}(X) \in \mathbb{R} \approx \mathrm{COP}(\min_{X \in \mathbb{R}^4} S_{gen}^{tot}(X) \in \mathbb{R}) \tag{40}$$

Compared to the optimal configuration corresponding to the maximization of the device's COP and the EGM, a slight difference is observed, mainly for the optimal number of channels (an approximately 8% difference) (Figs. 15 and 16). In fact, Fig. 17 shows that for a hot thermal power set to 55 W the range of channel numbers leading to the optimal COP is quite wide. This low sensitivity of the maximal COP to the number of channels explains that it is possible to have a variation of the optimal configuration between the two optimization methods without substantially varying the device's resulting optimal COP.

The optimization for given hot thermal power shows that there exists an optimal configuration of the heat exchangers and optimal mass flow for the hot and cold sides. The results also show that there is an optimal hot thermal power leading to the maximal optimal COP of the device. This last observation turns us to the following complete optimization, including the hot thermal power as a complementary variable.

4.2. Complete optimization

In this part, the hot thermal power demand is considered as an optimization variable in order to validate the optimal configuration obtained by partial optimization (29). Finally the optimization problem can be written:

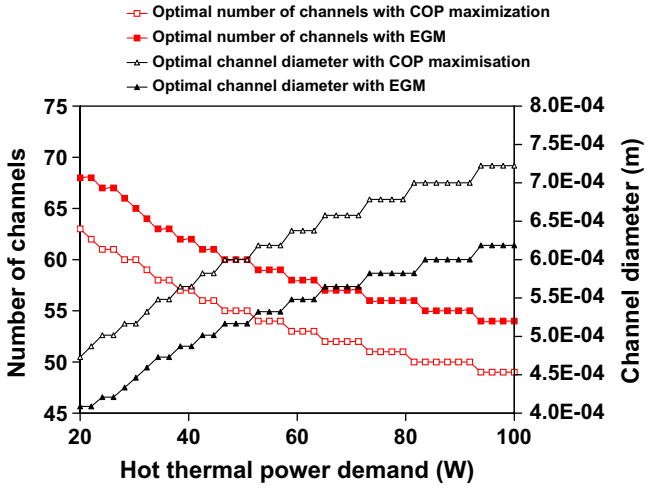

Fig. 15. Comparison of optimal geometries obtained by maximizing the device's COP and by EGM.

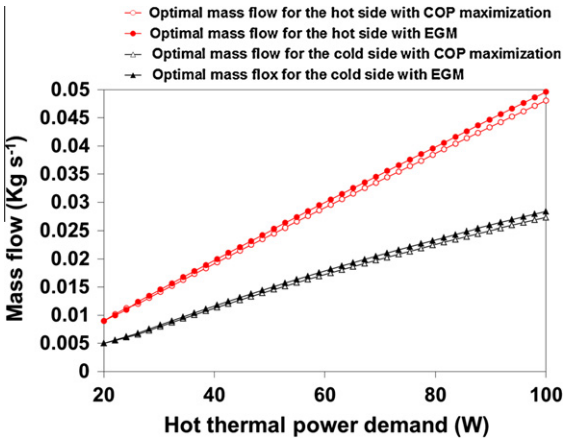

Fig. 16. Comparison of optimal mass flows obtained by maximizing the device's COP and by EGM.

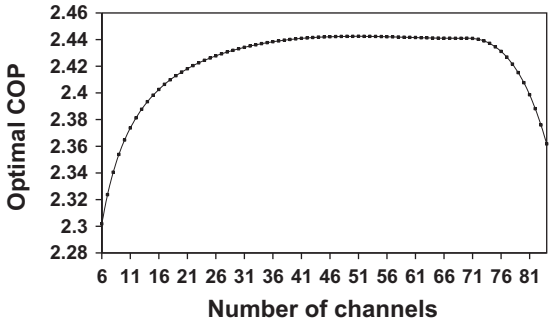

Fig. 17. Optimal COP of the device as a function of the number of channels for a thermal power demand of 55 W.

$$\max_{X\in\mathbb{R}^5} \mathrm{COP}_{device}(X) \in \mathbb{R} \tag{41}$$

$$X = (D^{ch},\ N^{ch},\ \dot{m}_c^{tot},\ \dot{m}_h^{tot},\ \phi_h) \tag{42}$$

The constraints are the same as for the previous cases ((33)).

For this optimization, the following results are obtained:

$D^{opt;ch} = 6.210^{-4}$ m; $N^{opt;ch} = 54$; $\dot{m}_h^{tot;opt} = 0.02629$ Kg s^{-1};
$\dot{m}_c^{tot;opt} = 0.01562$ Kg s^{-1}; $\phi_h^{opt} = 54.31$ W giving :

$\mathrm{COP}_{device}^{opt} = 2.44$; $R_h^{tot} = 0.04$ K W^{-1}; $R_c^{tot} = 0.02$ K W^{-1};
$\Delta P_h = 8050$ Pa; $\Delta P_c = 6170$ Pa

The optimal thermal power, the mass flows, the diameter and the number of mini-channels obtained with the complete optimization is the same as those obtained with the partial optimization.

Please note that, with complete optimization, including the thermal power as an optimization variable, the EGM criterion cannot be used. In fact, the minimum entropy generation of a thermal device is reached when the thermal power is minimal. Thus, according to the EGM criterion, the optimal operating condition is reached when the thermal power is null.

5. Conclusion

Thermoelectric heat pumps are an innovative technology for heating or cooling and show a high potential for low-consumption buildings. High thermal power can easily be reached by parallel association of the optimized unit presented in this paper. One of the most critical aspects of these devices is the many thermal resistances from the junctions of semi-conductors to the working fluid.

In this paper, an original configuration of a thermoelectric heat pump is introduced. The originality of this configuration comes from its compactness due to a thermal transfer on both sides of the central heat exchanger and to its modularity. In fact, this configuration provides two operating modes: TEM association in parallel or TEM association in cascade.

This paper focuses on the parallel operating mode. An analytical model was developed in order to completely optimize the device. The optimization criteria considered is the global COP including electrical consumption of the circulating auxiliaries.

The first part of the optimization introduced in this study highlights that an optimal heat exchanger design exists allowing one to maximize the device's global COP. In fact, when the hot thermal power demand increases, the optimal exchange area between the solid and the fluid increases as well. This increase is due to a decrease of the number of channels and an increase of their diameter due to a constant space between them. Concerning the optimal mass flow, an increase of its value is observed with the increase of the hot thermal power demand. Finally, when the hot thermal power increases, the optimal design (number of channels) and operating conditions associated (mass flow) increase the Reynolds number and thus the pressure drop and the heat transfer coefficient.

These results also show that for given fluid temperature conditions, there exists one optimal thermal power leading to the maximal COP.

The second result introduced in this paper is that it is possible to optimize the device by EGM. In fact, by minimizing this criterion, the same COPs are obtained by maximizing the device's global COP and by EGM. There is little variation of results concerning the corresponding optimal design due to the low sensitivity of the optimal COP to the number of channels within a large range.

Finally, it is possible to completely optimize the device, including the hot thermal power as an optimization variable. Consequently, we obtained an optimized device for given temperature conditions with the possibility of extending the thermal power generated with an association in parallel or in cascade without degrading the optimal COP.

In a future perspective, a flow distribution model must be added to take into account the pressure drop caused by the collection/distribution of water in the mini-channels. The optimized results may change with regard to the total pressure drop, including the collector/distributor, but the change may be slight as the mechanical consumption of the auxiliaries is two orders of magnitude below the electrical consumption of the thermoelectric modules.

Similarly, the estimation of the heat transfer coefficient must be improved. Optimized results may differ slightly.

References

[1] Seebeck TJ. Magnetische Polarisation des Metalle und Erz durch Temperaturdifferentz. Berlin: Abhandlungen der deutshen akademie der Wissenschaften zu; 1822.
[2] Thomson W. On a mechanical theory of thermoelectric currents. Royal Society; 1851.
[3] Peltier J. Nouvelles expériences sur la caloricité des courants électriques. Ann Chem Phys 1834;56:371–87.
[4] Stockholm JG. Génération thermoélectrique. Cachan, France: Journées Electrotechniques du Club EEA; 2002.
[5] Telkes M. The efficiency of thermoelectrique generators. Int J Appl Phys 1947;18:1116–27.
[6] Vining CB. Semiconductors are cool. Nature 2001;413:77–578.
[7] Min G, Rowe DM. Improved model for calculating the coefficient of performance of a Peltier module. Energy Convers Manage 2000;41:163–71.
[8] Lee KH, Kim OJ. Analysis on the cooling performance of the thermoelectric micro-cooler. Int J Heat Mass Transfer 2007;50:1982–92.
[9] Omer SA, Infield DG. Design optimization of thermoelectric devices for solar power generation. Sol Energy Mater Sol Cells 1998;53:67–82.

[10] Chein R, Chen Y. Performances of thermoelectric cooler integrated with microchannel heat sinks. Int J Refrig 2005;28:828–39.
[11] Rosengarten G, Mutzenich S, Kalantar-zadeh K. Integrated microthermoelectric cooler for microfluidic channels. Exp Therm Fluid Sci 2006;30:821–8.
[12] Crane DT, Jackson GS. Optimization of cross flow heat exchangers for thermoelectric waste heat recovery. Energy Convers Manage 2004;45:1565–82.
[13] Khire RA, Messac A, Van Dessel S. Design of thermoelectric heat pump unit for active building envelope systems. Int J Heat Mass Transfer 2005;48:4028–40.
[14] David B, Ramousse J, Luo L. Optimization of a thermoelectric heat pump for the heating and cooling of sustainable buildings. CLIMA2010, Antalya, Turquie; ; 2010. p. 25–6.
[15] Rowes DM, editor. CRC handbook of thermoelectrics. C. Press; 1995.
[16] FERROTEC. Ferrotec manufactures component, material, and system solutions for a broad range of precision products and industries; 2012. <http://thermal.ferrotec.com/index.php?id=module_detail&mod_id=118>.
[17] Kikas NP. Laminar flow distribution in solar systems. Fuel Energy Abstr 1995;54:209–17.
[18] Saber M, Commenge JM, Falk L. Rapid design of channel multi-scale networks with minimum flow maldistribution. Chem Eng Process: Process Intens 2009;48:723–33.
[19] Tondeur D, Fan Y, Commenge JM, Luo L. Flow and pressure distribution in linear discrete ''ladder-type'' fluidic circuits: an analytical approach. Chem Eng Sci 2011;66:568–2586.
[20] Tondeur D, Fan Y, Commenge JM, Luo L. Uniform flows in rectangular lattice networks. Chem Eng Sci 2011;66:5301–12.
[21] Tondeur D, Fan Y, Luo L. Flow distribution and pressure drop in 2D meshed channel circuits. Chem Eng Sci 2011;66:15–26.
[22] Shah RK, London AL. Laminar flow forced convection in ducts. S.t.A.i.H. Transfer, editor. New York: Academic Press; 1978.
[23] Ritzer TM, Lau PG. Economic optimization of heat sink design. In: 13th International conference on thermoelectrics, Kansas, City; 1994.
[24] Langhaar HL. J Appl Mech 1942;64:55–8.
[25] Shah RK. Thermal entry length solutions for the circular tube and parallel plates. Heat Mass Transfer Conference. Bombay: Indian Inst. Technol.; 1975.
[26] Darcy H. Recherches expérimentales relatives au mouvement de l'eau dans les tuyaux. Mallet-Bachelier; 1857.
[27] Weisbach J. Lehrbuch der Ingenieur- und Maschinen-Mechanik; 1845.
[28] Tondeur D, Fan Y, Luo L. Constructal optimization of arborescent structures with flow singularities. Chem Eng Sci 2009;64:3968–82.
[29] Lewis RM, Torczon V, Trosset MW. Direct search methods: then and now. Institute for Computer Applications in Science and Engineering, Hampton, Virginia, vol. 26; 2000.
[30] Bejan A. Method of entropy generation minimization, or modeling and optimization based on combined heat transfer and thermodynamics. Revue Générale Therm 1996;35:637–46.
[31] Khan WA, Yovanovich MM, Culham JR. Culham, Optimization of microchannel heat sinks using entropy generation minimization method, Semiconductor thermal measurement and management symposium. Texas: Dallas; 2006.
[32] Chen L, Wu C, Sun F. Heat transfer effect on the specific cooling load of refrigerators. Appl Therm Eng 1996;16:989–97.
[33] Göktun S. Design considerations for a thermoelectric refrigerator. Energy Convers Manage 1995;36:1197–200.
[34] Bejan A. General criterion for rating heat exchanger performance. Int J Heat Mass Transfer 1978;21:655–8.